

# Three-Dimensional Structure-Activity Analysis of a Series of Porphyrin Derivatives with Anti-HIV-1 Activity Targeted to the V3 Loop of the gp120 Envelope Glycoprotein of the Human Immunodeficiency Virus Type 1

Asim Kumar Debnath,\*† Shibo Jiang,† Nathan Strick,† Kang Lin,† Paul Haberfield,‡ and A. Robert Neurath†

The Lindsley F. Kimball Research Institute of the New York Blood Center, New York, New York 10021, and Department of Chemistry, Brooklyn College of the City University of New York, Brooklyn, New York 11210

Received December 13, 1993\*

Using comparative molecular field analysis (CoMFA), a 3D-QSAR model was developed for 21 porphyrin derivatives which have anti-HIV-1 activity and bind to the V3 loop of the envelope glycoprotein gp120 of the human immunodeficiency virus type 1. A significant PLS cross-validated  $r^2_{cv}$  (0.590) was obtained, indicating that the model could be used as a predictive tool for further design of porphyrin analogs. The model revealed at least three important sites for favorable electrostatic interactions and indicated favorable and unfavorable steric interaction sites. It was found that the occurrence of at least three positively charged and several hydrophobic amino acid residues is highly conserved at fixed positions of gp120 V3 loop sequences. This may support the validity of the proposed model and the hypothesis that porphyrins containing anionic and hydrophobic groups may interact with some of the highly conserved positively charged and hydrophobic sites, respectively, of the V3 loop. These interactions may induce conformational changes in the gp120 envelope glycoprotein leading to inhibition of virus entry into cells and of syncytium formation (cell-to-cell fusion) and thus to inhibition of virus replication.

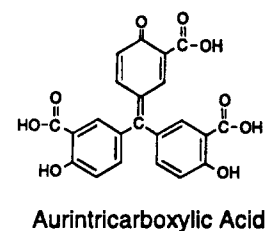
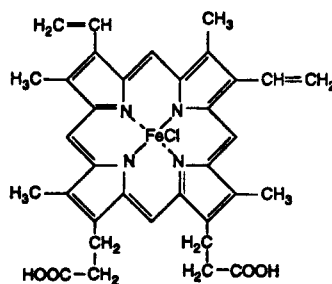
## Introduction

Effective treatments against human immunodeficiency virus type 1 infection are of utmost importance worldwide. 3'-Azido-3'-deoxythymidine (AZT) has been the anti-HIV-1 drug of choice for some time. However, there are some major concerns about AZT, i.e., emergence of AZT-resistant variants and serious toxic effects.<sup>1-6</sup> The promise of AZT has become questionable based on results of an European clinical trial, known as Concorde, indicating that AZT offered little benefit in the early stage of HIV infection.<sup>7</sup> The introduction of 2',3'-dideoxyinosine (ddI) and 2',3'-dideoxycytidine (ddC) has increased the arsenal of anti-HIV-1 drugs. However, these three nucleoside analogs are all targeted to the same enzyme, reverse transcriptase (RT). The clinical experience with AZT strongly calls for additional targets for anti-HIV drug development. Toward this goal our group and others have reported alternative targets for anti-HIV therapy.<sup>8-14</sup>

Binding of the envelope glycoprotein gp120 to the CD4 cell receptor is thought to be necessary but not sufficient for viral entry in the initial step of the HIV replication cycle.<sup>15,16</sup> Mouse cells transfected with the CD4 gene and expressing the CD4 cell surface protein were resistant to HIV-1 infection, suggesting that the block of infection most likely occurred at a stage involving virion-cell fusion after the binding of HIV-1 virions to CD4.<sup>15</sup> Site-directed mutagenesis experiments suggested an important role of defined gp120 segments in the fusion process. Some amino acid replacements within the third hypervariable region, known as the V3 loop, of gp120 rendered the envelope glycoprotein fusion-defective.<sup>17,18</sup> A principal virus neutralizing determinant (PND) was also found to be located in the V3 loop region, and antibodies recognizing the PND effectively blocked virus infectivity and syncytium forma-

tion (i.e., cell-to-cell fusion).<sup>19-21</sup> The critical nature of the V3 loop suggests that this region of gp120 could be a potential target site for anti-HIV-1 agents.

A rapid prescreening method for anti-HIV-1 agents based on their inhibitory activity in site-directed immunoassays, measuring the attachment to gp120 of antibodies specific for the V3 loop of this envelope glycoprotein, has been developed.<sup>8,22</sup> One of the substances identified by this prescreening method was hemin, reported earlier to inhibit the replication of HIV-1.<sup>23</sup> Several porphyrin derivatives were more potent inhibitors of HIV-1 replication than hemin or aurotricarboxylic acid (ATA).<sup>8</sup> The latter compound also inhibited the attachment to gp120 of antibodies specific for the V3 hypervariable loop.<sup>22</sup> This finding and the availability of a multitude of porphyrin derivatives prompted us to study their anti-HIV-1 activity and establish a quantitative structure-activity relationship (QSAR).



In this report we present the application of comparative molecular field analysis (CoMFA) for the development of a 3D QSAR model for porphyrins with anti-HIV-1 activity.

## Experimental Section

Propionic acid was fractionated through a 5-cm Vigreux column. The fraction with bp 139-140 °C was collected. Tolualdehyde was fractionated through a 10-cm Vigreux column

\* Author to whom all correspondence should be addressed.

† New York Blood Center.

‡ Brooklyn College of the City University of New York.

• Abstract published in *Advance ACS Abstracts*, March 15, 1994.

at 2 mm of pressure. The fraction with bp 56–57 °C was isolated. Pyrrole was distilled at atmospheric pressure under an argon atmosphere (bp 132 °C). *p*-Carboxybenzaldehyde was obtained from Aldrich, Milwaukee, WI, and was used as is. TLC's were run on Macherey Nagel silica gel G plates. Column chromatography was done on Merck silica gel 60 (230–400-mesh flash silica). Bruker 250- and 300-MHz spectrophotometers were used for <sup>1</sup>H NMR. IR spectra were measured with a Mattson FTIR spectrophotometer as a Nujol mull. The visible absorption spectrum was measured on a Cary 1 UV/vis spectrophotometer. Mass spectra were determined on a Kratos M580RFA spectrometer operating in the FAB mode.

Compounds 17–19 and 21 were synthesized by Porphyrin Products, Logan, UT (numbering and structures of the compounds are shown in Figure 2).<sup>24–26</sup> All other compounds (except 14 and 20) are commercially available from Porphyrin Products.

**2,9,16,23-Tetraaminophthalocyanine (14).** 2,9,16,23-Tetranitrophthalocyanine was prepared following a modified procedure used by Achar *et al.*<sup>27</sup> 4-Nitrophthalic acid (37.0 g, 175 mmol), urea (55 g, 917 mmol), ammonium chloride (4.5 g, 85 mmol), and ammonium molybdate (0.5 g, 0.4 mmol) were stirred vigorously in 25 mL of nitrobenzene at 185 °C for 4.5 h. The product was filtered and the solid washed with ethanol. The solid was next boiled for about 5 min in 0.5 L of 1.0 N hydrochloric acid saturated with NaCl (200 g) until the evolution of ammonia ceased, and the mixture was filtered. This treatment, alternately with HCl and NaOH, was repeated twice. The product was then washed with water and dried. The yield was 2.2 g (7.2%): <sup>1</sup>H NMR (DMSO) δ 8.25 (m, 4H), 7.85 (m, 4H), 7.70 (m, 4H).

2,9,16,23-Tetraaminophthalocyanine was prepared by reduction of the above nitro compound. 2,9,16,23-Tetranitrophthalocyanine (2.0 g, 2.88 mmol) and sodium sulfide nonahydrate (10 g, 41.6 mmol) were stirred in 50 mL of water at 50 °C for 5 h. The product was separated by filtration and washed successively with water until it was free of sodium hydroxide and sodium chloride. It was then dried, yielding 0.87 g (53%) of a dark blue powder soluble in concentrated hydrochloric acid, DMSO. TLC showed a single spot on silica gel using two different solvent systems [*R<sub>f</sub>* = 0.79 (DMF); *R<sub>f</sub>* = 0.69 (50 vol % DMF/CH<sub>3</sub>COCH<sub>3</sub>)]: <sup>1</sup>H NMR (DMSO) broad bands at approximately δ 7.5, 6.7, and 6.5.

**5-(*p*-Carboxyphenyl)-10,15,20-tritolyldorphine (20).** The compound was synthesized by the mixed aldehyde approach of Anton *et al.*<sup>28</sup> Propionic acid (700 mL) was heated to reflux under an argon atmosphere. Toluualdehyde (18.0 g, 0.15 mol) and *p*-carboxybenzaldehyde (4.5 g, 0.03 mol) were added to the magnetically stirred solution. After the solution had returned to reflux, pyrrole (12.1 g, 0.18 mol) was added dropwise over 10 min. A violent reaction occurred and the solution became dark brown. Reflux was continued for another 30 min. The reaction mixture was cooled to room temperature and refrigerated for 24 h. The mixture was filtered, and the purple crystalline solid obtained was washed with 3 × 20 mL of methanol, 2 × 15 mL of hot water, and 1 × 10 mL of methanol. It was then dried *in vacuo* at room temperature for several hours; 5.5 g of material was isolated. TLC (CHCl<sub>3</sub>) showed two major spots with *R<sub>f</sub>* 0.85 and 0.07. There were also several minor spots, one of which remained at the origin.

The crude product mixture was partially dissolved in 125 mL of chloroform and applied to a 26 × 6.5-cm column of silica gel 60 (400 g) packed in chloroform. The column was first eluted with chloroform. Fractions of 125 mL were collected. Chloroform was added to the column in 125-mL portions to concentrate the material in as narrow a band as possible. The initial colorless chloroform eluate was recycled back onto the column. A deep purple-red solution of the tetratolyldorphine eluted first. After five fractions had been collected, the eluting solvent was changed to chloroform-methanol (20:1). The tetratolyldorphine was collected in a total of 12 fractions. A thin black impurity band eluted in the next two fractions. This was followed by a reddish purple solution of the product in fractions 21–28. They were combined and the solvent was evaporated yielding the product as a reddish purple powder. TLC (CHCl<sub>3</sub>-MeOH, 10:1) showed only one spot with *R<sub>f</sub>* = 0.45. The compound was 99% pure by HPLC analysis (4.6-mm × 25-cm Dupont Zorbax 5 μm silica; isocratic elution with 10:1 (v/v) CHCl<sub>3</sub>-CH<sub>3</sub>OH at 0.6 mL/min; UV/visible detection at 420 nm); UV λ<sub>max</sub> (in benzene) 420, 515,

551, 590, and 649 nm; IR 1639 cm<sup>-1</sup> (COOH); <sup>1</sup>H NMR (CDCl<sub>3</sub>) δ 2.70 (s, 3H, methyl), 2.77 (s, 3H, methyl); FAB-MS *m/e* 700.0 (M), 701.0 (M + H).

**Antiviral Activity.** Inhibition of HIV-1 replication by porphyrin derivatives was determined by enzyme-linked immunoadsorbent assays (ELISA) measuring HIV-1 core protein P24 production as reported earlier.<sup>29</sup> Briefly, MT-2 cells were infected with HIV-1 IIIB (multiplicity of infection = 0.0045) in the presence or absence of the porphyrin derivatives. On the fourth day of incubation at 37 °C, culture supernatants were collected and assayed for P24 using a kit from Coulter Immunology (Hialeah, FL). The percentage of inhibition of P24 production and EC<sub>50</sub> were calculated as described before.<sup>8,29</sup> Though some of the activity data on the porphyrin derivatives were reported earlier,<sup>8</sup> all compounds were retested and the EC<sub>50</sub> data were pooled from previous and current tests, and mean values along with standard deviations (SD) expressed in micromolar concentrations are reported here and used as the biological activity parameter for the QSAR-CoMFA study.

## Molecular Modeling

All molecular modeling was done using Sybyl 6.01 of Tripos Associates, Inc., St. Louis, MO, running on an IBM/RISC 6000.<sup>30</sup>

**Conformational Analysis and Geometry Optimization.** The starting geometries of protoporphyrin IX (1), *N*-methylprotoporphyrin IX (2), mesoporphyrin IX (4), deuteroporphyrin IX, 2-(hydroxyethyl)-4-vinyl- (5), deuteroporphyrin IX, 2-vinyl-4-(hydroxymethyl)- (6), deuteroporphyrin IX, 2,4-bisglycol (7), uroporphyrin III (8), uroporphyrin I (9), pentacarboxylporphyrin I (10), hexacarboxylporphyrin I (11), and heptacarboxylporphyrin I (12) were constructed from the crystal structure of protoporphyrin IX dimethyl ester<sup>31</sup> using the "Built/Edit" option of Sybyl 6.01.

The chlorin e<sub>6</sub> (13) starting geometry was built from the crystal structure of methyl pheophorbide.<sup>32</sup> The ethyl and vinyl groups of chlorin e<sub>6</sub> were oriented similarly to the two vinyl groups of protoporphyrin IX (1).

2,9,16,23-Tetraaminophthalocyanine (14) was constructed based on the X-ray crystallographic structure of phthalocyanine.<sup>33</sup>

In the case of *meso*-tetraphenylporphyrin compounds (15–21), four phenyl groups on the *meso* carbon atoms were oriented 60° out of plane based on the crystal structure of *meso*-tetraphenylporphyrin.<sup>34</sup>

The geometries of all 21 compounds were optimized with MAXIMIN2 of Sybyl 6.01 using the Tripos force field.<sup>35</sup> The default settings were used. Gasteiger-Marsili charges were used for energy minimization.

Twelve protoporphyrin IX type compounds (see Figure 2, 1, 2, 4–13) were initially selected for extensive conformational searches using the "systematic search" option within Sybyl 6.01. The active analog approach<sup>36,37</sup> was used to reduce the enormous number of possible conformations to a manageable number of conformations common to all these molecules. A distance map consisting of two distance ranges was created using three pharmacophore site points on each molecule as shown in Figure 1. Protoporphyrin IX (1) was considered as the reference molecule for building our "active-site hypothesis". This decision was made independently of any QSAR data obtained in the course of this study. We considered a qualitative structure-activity relationship for all 12 molecules, representing the majority of the compounds in this study and including protoporphyrin IX (1) which is one of the most active compounds in this series. One of the OH "O" of propionic acid was considered as the active site

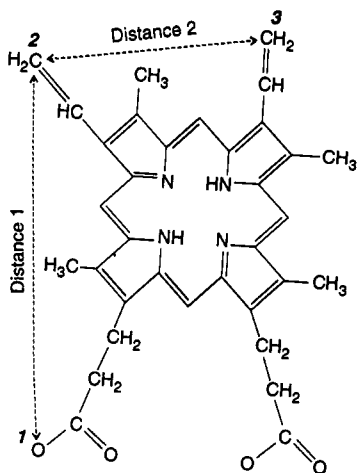


**Figure 1.** Distance map consisting of two distance ranges and three pharmacophore site points used for conformational search [protoporphyrin IX (1) is shown as an example].

for binding with one of the positively charged amino acids of the V3 loop. Two vinyl end carbons were also considered as the pharmacophore site points for possible steric/hydrophobic effects. The equivalent atoms for all the rest of the compounds were considered for building the distance map for systematic search.

The conformational searches were performed using a 60° torsional increment in the torsional space. This relatively coarse search had to be opted for since the molecules considered had as many as 28 rotatable bonds and could generate an unmanageable number of conformations. All bonds which might influence the conformation of the pharmacophore site points were rotated (as shown in Figure 2). The rest of the bonds were kept fixed at the torsion angles found after initial MAXIMIN2 minimization.

Though, initially, 12 structures were selected for conformational search, only eight structures were used as shown in Table 1. The use of the uroporphyrin III (8) distance map for constraining the conformational searches of either uroporphyrin I (9), pentacarboxylporphyrin I (10), hexacarboxylporphyrin I (11), or heptacarboxylporphyrin I (12) did not reduce the number of conformations to a manageable number. Therefore, these four compounds were omitted and a different technique was used for the conformational search as discussed below.

The distance map for the eighth molecule (i.e., uroporphyrin III) was used to constrain a second conformation search on all the eight compounds. The results are shown in Table 1. An energy cutoff of 4.0 kcal/mol using Gasteiger–Marsili charges was used along with distance map constraints to further reduce the conformations.

A family classification using the distance ranges from the final distance map generated only one family for each molecule (0.2-Å grid size). The minimum-energy conformation for each family was selected for further geometry optimization.

The final distance map of the minimum-energy conformation of protoporphyrin IX (1) from the conformational search was used as the distance constraint for the conformational searches of the rest of the four molecules with the most rotatable bonds, e.g., uroporphyrin I (9), pentacarboxylporphyrin I (10), hexacarboxylporphyrin I (11), and heptacarboxylporphyrin I (12). The minimum-energy structures in each case were selected for further analysis.

The minimum-energy conformation of protoporphyrin IX (1) was modified by replacing H of two COOH groups with CH<sub>3</sub> to construct the structure of protoporphyrin IX, dimethyl ester (3).

All 21 molecules were then subjected to energy minimization using MAXIMIN2 of Sybyl 6.01. Tripos force field, Gasteiger–Marsili charges were used. These structures were optimized completely using the semiempirical method AM1<sup>38</sup> of MOPAC 5.0 adapted to Sybyl 6.01. The keywords “BONDS”, “XYZ”, “NOINTER”, “VECTOR”, and “PRECISE” were used in all cases. Whenever the results did not pass the “gradient test”, the keyword “NLLSQ” was used to lower the gradient. The keyword “MMOK” was used for molecular mechanics correction for amidic bonds. The MOPAC charges were used to calculate the electrostatic interactions in CoMFA.

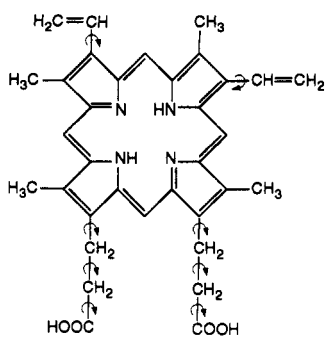
**Alignment Rule.** Protoporphyrin IX (1) was selected as the reference molecule for alignment, since the majority of the compounds studied belonged to this class and 1 was one of the most active compounds tested. All other protoporphyrin IX type structures (2–13) and 2,9,16,23-tetraaminophthalocyanine (14) were superimposed on the four meso carbon atoms of the reference molecule in such a way that it satisfied the proposed pharmacophore site point hypothesis used to perform conformational searches. All tetraphenylporphyrin type compounds were superimposed on the reference molecule so that one of their carboxylic acid OH lies near the propionic acid OH of the reference molecule. Two of the phenyl groups were also aligned in such a fashion that they also lay near the two vinyl groups of protoporphyrin IX used as pharmacophore site points. Figure 3 shows the superimposed structures of the 21 porphyrin derivatives tested and used to derive the 3D-QSAR model.

### CoMFA Analyses

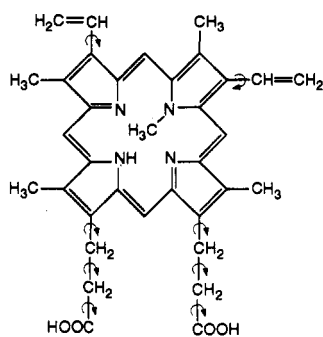
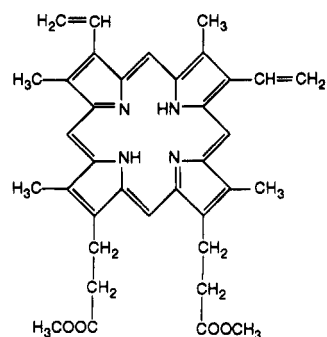
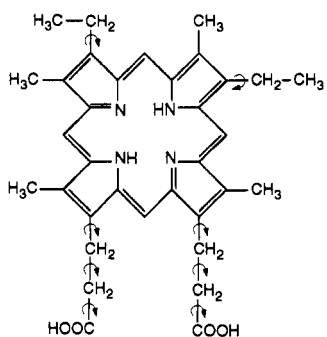
The CoMFA analyses were carried out using the QSAR module of Sybyl 6.01. The aligned compounds were placed within a grid box containing equally spaced lattice points (2 Å). A specific probe atom (Csp<sup>3</sup>) with well-defined characteristics was placed at each lattice intersection. The noncovalent interaction energies (steric and electrostatic) were then calculated for aligned compounds. The correlation of these noncovalent interaction energies with the target property was then sought using the partial least squares (PLS) technique.<sup>39</sup> The “best” predictive model was then derived from the leave-1-out cross-validation test.<sup>40</sup> The final CoMFA model was built using the same number of components (often called latent variables) identified by the cross-validation test but using no cross-validation. The results were then analyzed by using contour plots.

### Interaction Energy Calculations

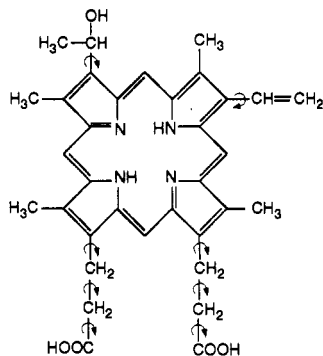
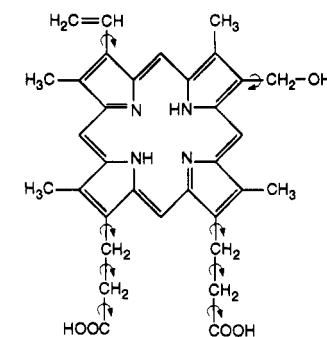
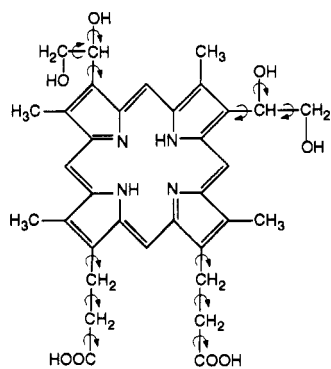
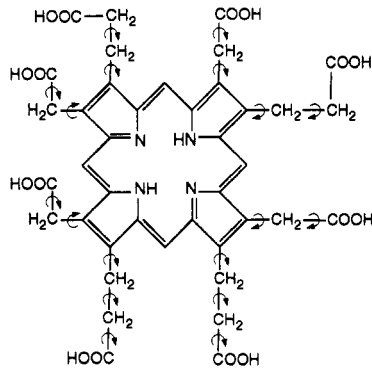
The steric and electrostatic potential energy fields of each molecule were calculated at various lattice points surrounding the molecule using the Lennard–Jones and Coulombic potential function, respectively, within the Tripos force field<sup>35</sup> using a Csp<sup>3</sup> probe with a +1.0 charge. This probe has no hydrogen bond donating or accepting properties. The partial atomic charges calculated using AM1 of MOPAC 5.0 were used for calculating electrostatic interactions. The gridbox dimensions for CoMFA analyses were determined using the “create automatically” feature of the Sybyl/CoMFA program. This ensured that the



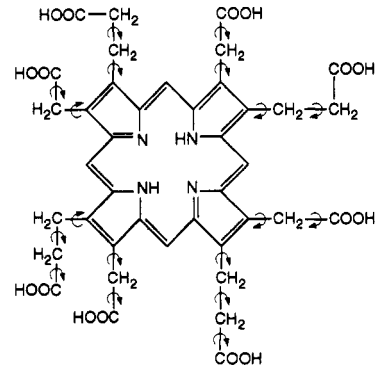
Protoporphyrin IX (#1)

N-methyl  
protoporphyrin IX (#2)Protoporphyrin IX  
dimethyl ester (#3)

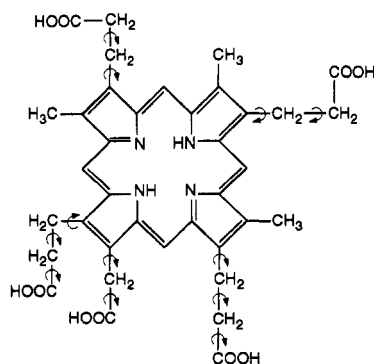
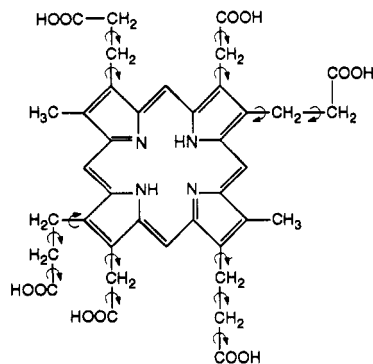
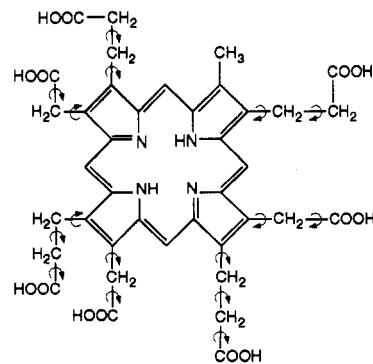
Mesoporphyrin IX (#4)

Deuteroporphyrin IX, 2-  
hydroxyethyl-4-vinyl- (#5)Deuteroporphyrin IX,  
2-vinyl 4-hydroxymethyl- (#6)Deuteroporphyrin IX  
2,4-bisglycol (#7)

Uroporphyrin III (#8)



Uroporphyrin I (#9)

Pentacarboxyl  
porphyrin I (#10)Hexacarboxyl  
porphyrin I (#11)Heptacarboxyl  
porphyrin I (#12)

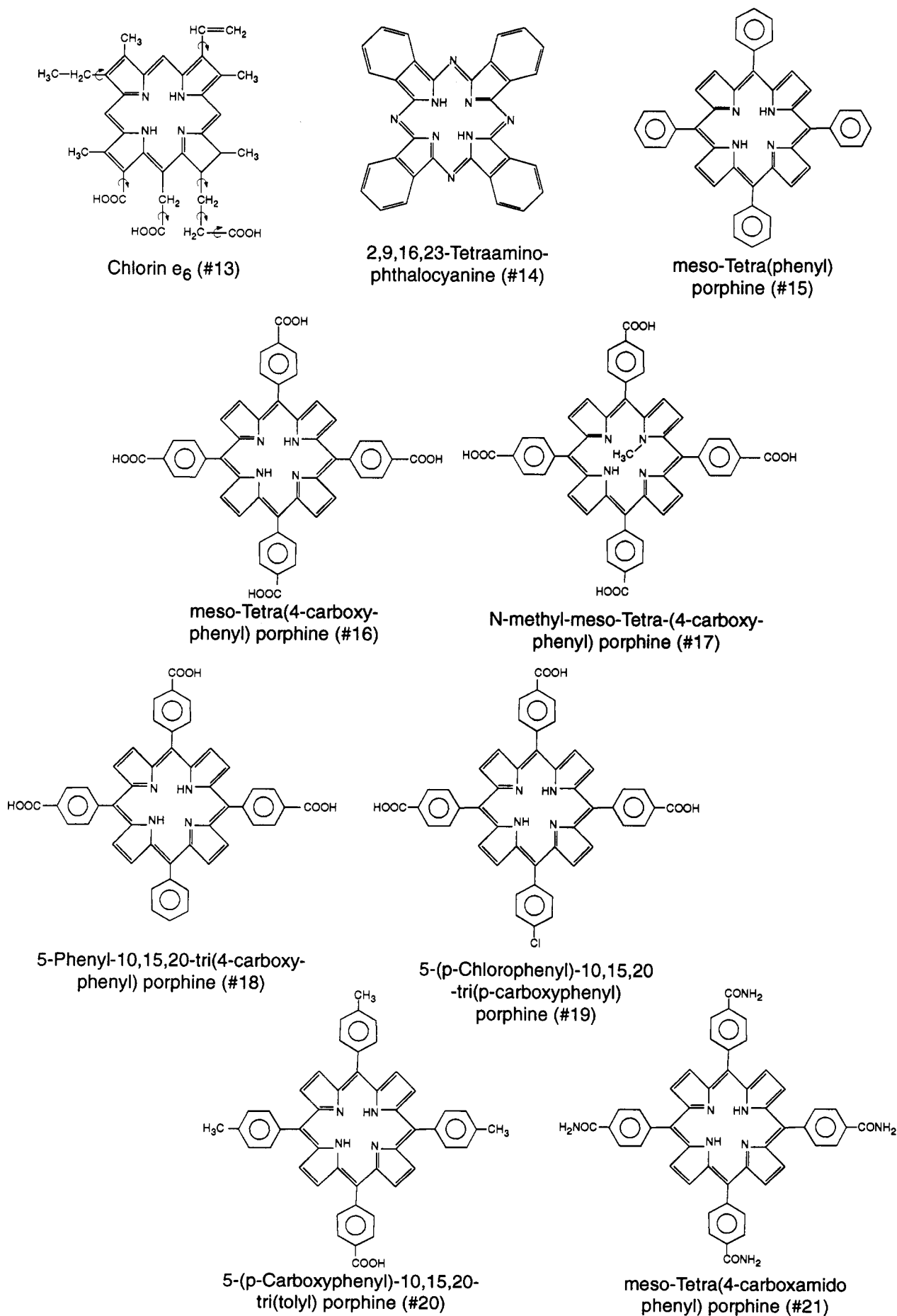


**Figure 2.** Structures of porphyrin analogs used to derive the 3D-QSAR model. The curved-arrow symbol ( $\curvearrowright$ ) indicates the bonds used for scanning torsional space in the "systematic search". "#" corresponds to boldface numbers in the text and in Table 4.

**Table 1.** Systematic Conformational Search Using the "Active Analog" Approach

no.	compound name	1st systematic search			2nd systematic search		
		compd used as constraint for distance map	no. of distance map data points	no. of conformations	compd used as constraint for distance map	no. of distance map data points	no. of conformations
1	protoporphyrin IX	no	209	14480	8	2	141
2	<i>N</i> -methylprotoporphyrin IX	1	123	9507	8	2	53
3	mesoporphyrin IX	2	36	2101	8	2	38
4	deuteroporphyrin IX,	3	19	916	8	2	62
	2-(hydroxyethyl)-4-vinyl-						
5	deuteroporphyrin IX,	4	7	490	8	2	57
	2-vinyl-4-(hydroxymethyl)-						
6	Chlorin $e_6$	5	5	1376	8	2	194
7	deuteroporphyrin IX, 2,4-bisglycol	6	5	224	8	2	57
8	uroporphyrin III	7	2	286	8	2	31

**Table 2.** Parameters and Statistics of Cross-Validated PLS-CoMFA<sup>a</sup>

statistics	components				
	1	2	3	4 <sup>b</sup>	5
$r^2_{cv}$	0.163	0.285	0.526	0.590	0.567
$S_{cv}$	0.634	0.603	0.507	0.486	0.517

<sup>a</sup> Minimum  $\sigma$ : 2.0. Leave-1-out cross-validation runs: 20. <sup>b</sup> Selected components.

**Table 3.** Parameters and Statistics of the "Fitted Model" by PLS-CoMFA

parameters	statistics
minimum $\sigma$ : 0.0	$r^2 = 0.979$
number of components used: 4	$S = 0.109$
cross-validation runs: 0	$F \text{ value} = 178.4$

"region" (or the gridbox) boundaries were extended beyond 4 Å in each direction from the coordinates of every molecule. The starting gridbox dimension created by this method was 29.8 × 29.8 × 16.4 (X = -22.7 to 7.1, Y = -12.7 to 17.1 and Z = -7.5 to 8.9) with 2-Å lattice spacing. An energy cutoff of 4.0 kcal/mol was set for both steric and electrostatic interactions.

**Partial Least Squares (PLS) Calculations.** Five orthogonal latent variables were first extracted by the standard PLS algorithm<sup>39</sup> using the starting lattice position. The latent variables were subjected to the leave-1-out cross-validation test in the original order of extraction. The minimum  $\sigma$  value was set to 2.0, and CoMFA scaling was set to CoMFA-Standard. The best "predictive" model (Table 2) with the "optimum number" of components was chosen from the lowest value of the cross-validated standard error of estimate ( $S_{cv}$ ) which is defined as<sup>41</sup>

$$S_{cv} = \sqrt{\frac{\text{PRESS}}{n - c - 1}}$$

where

$$\text{PRESS} = \sum_Y (Y_{\text{Pred}} - Y_{\text{Act}})^2$$

and  $n$  = number of rows (i.e., data points),  $c$  = number of components.

The "best" correlation model (fitted model) was derived using no cross-validation with the optimum number of components. A minimum  $\sigma$  value of 0.0 and CoMFA scaling of "none" were used (Table 3).

## Results

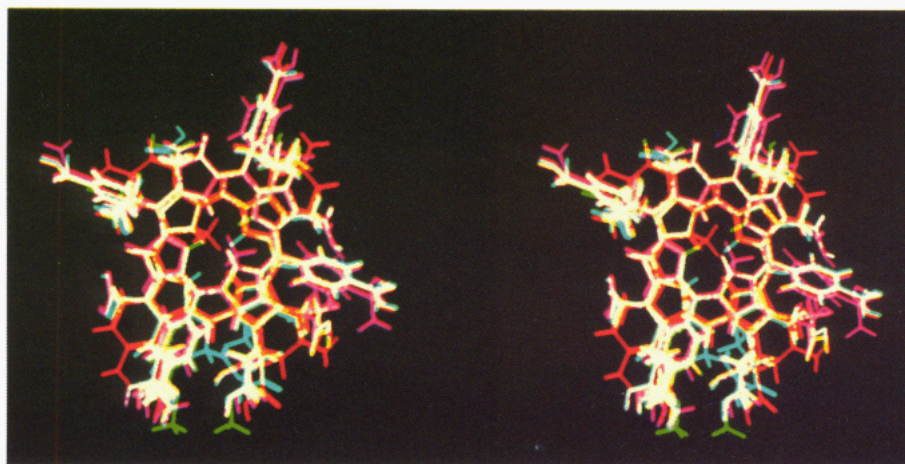
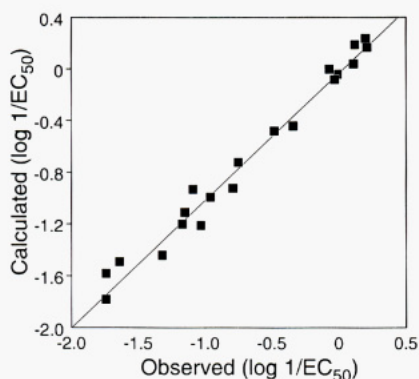
The compounds used for this study, their anti-HIV-1 activity ( $EC_{50}$ ) expressed in micromolar concentrations,

the calculated anti-HIV-1 activity using the "fitted model", and the deviation from the observed value are shown in Table 4. The leave-1-out cross-validation test with all 21 compounds resulted in a cross-validated  $r^2_{cv}$  of 0.424 with a cross-validated standard error of estimate ( $S_{cv}$ ) of 0.579. This test identified one compound as an outlier (3). Protoporphyrin IX dimethyl ester (3) has very poor solubility, which might have caused problems in determining anti-HIV-1 activity. When this compound was omitted from the analysis, the cross-validated  $r^2_{cv}$  improved considerably ( $r^2_{cv} = 0.590$ ). This leave-1-out cross-validation test with 20 compounds had identified four optimal components out of five extracted (Table 2). The "best" correlation model was derived using four components and other parameters were set as detailed in Table 3. This model resulted in a correlation coefficient explaining 98% of the total variance in anti-HIV-1 activity with a standard error of estimate ( $S$ ) of 0.109. Component 1 explained 45% of the total variance while adding components 2, 3, and 4 explained 42%, 12%, and 4%, respectively. Electrostatic interaction is the major contributing factor (64%) toward explaining anti-HIV-1 activity, whereas steric factors contributed 36%. Both percent variance and contributions are obtained from the QSAR report using Sybyl 6.01. Figure 4 shows a plot of observed vs calculated anti-HIV-1 activity using the "fitted model". Three-dimensional contour plots were also derived from this model. The usefulness of these contour plots are 2-fold. They not only identify important regions where any change in the steric or electrostatic fields may affect the target property but they might also contribute to the identification of important interaction sites on the receptor. The coefficient contour plot of the electrostatic fields is shown in Figure 5. The contour shows that more negative charge near the red region increases potency whereas more negative charge near the blue region decreases potency. The contour was drawn at a 0.005 level. The coefficient contour plot of the steric field is shown in Figure 6. Positive contours (green) have a favorable steric effect and increase the predicted antiviral activity, while negative contours (yellow) have an unfavorable steric effect and decrease the activity. The contour was drawn at a 0.007 level. The positive contours in Figure 6 could be interpreted as regions for favorable steric and/or hydrophobic interactions, i.e., increase of bulk in the positive contour regions, especially hydrocarbons or phenyl rings, is expected to increase antiviral activity. The above analyses were repeated with a grid spacing of 1 Å and resulted in slightly poorer correlations ( $r^2_{cv} = 0.584$  and  $S_{cv} = 0.490$ ;  $r^2 = 0.969$  and  $S = 0.133$ ). A lattice position shift by -0.5, -1.0, and -1.5 Å from the starting position

**Table 4.** Observed and Calculated Anti-HIV-1 Activities of Porphyrin Derivatives<sup>a</sup>

no.	compound	EC <sub>50</sub> , μM <sup>c</sup> (±SD)	log 1/EC <sub>50</sub>		
			observed	calculated	difference
1	protoporphyrin IX	2.170(0.362)	-0.34	-0.44	0.10
2	<i>N</i> -methylprotoporphyrin IX	1.030(0.343)	-0.01	0.04	-0.05
3 <sup>b</sup>	protoporphyrin IX dimethyl ester	67.874(15.460)	-1.83	-0.47	-1.36
4	mesoporphyrin IX dihydrochloride	14.057(2.708)	-1.15	-1.11	-0.05
5	deuteroporphyrin IX, 2-(hydroxyethyl)-4-vinyl-	6.163(0.606)	-0.79	-0.92	0.13
6	deuteroporphyrin IX, 2-vinyl-4-(hydroxymethyl)-	5.589(1.018)	-0.75	-0.72	-0.03
7	deuteroporphyrin IX, 2,4-bisglycol	54.411(8.319)	-1.74	-1.58	-0.16
8	uroporphyrin III dihydrochloride	3.018(0.854)	-0.48	-0.48	0.00
9	uroporphyrin I dihydrochloride	9.037(2.576)	-0.96	-0.99	0.03
10	pentacarboxylporphyrin I dihydrochloride	43.317(7.417)	-1.64	-1.49	-0.15
11	hexacarboxylporphyrin I dihydrochloride	20.686(1.702)	-1.32	-1.44	0.12
12	heptacarboxylporphyrin I dihydrochloride	10.724(2.205)	-1.03	-1.21	0.18
13	chlorin <i>e</i> <sub>8</sub>	1.174(0.341)	-0.07	0.00	-0.07
14	2,9,16,23-tetraaminophthalocyanine	12.276(0.703)	-1.09	-0.93	-0.16
15	<i>meso</i> -tetraphenylporphine	54.708(5.518)	-1.74	-1.78	0.04
16	<i>meso</i> -tetrakis(4-carboxyphenyl)porphine	0.630(0.166)	0.20	0.24	-0.04
17	<i>N</i> -methyl- <i>meso</i> -tetrakis(4-carboxyphenyl)porphine	0.774(0.160)	0.11	0.04	0.07
18	5-phenyl-10,15,20-tris( <i>p</i> -carboxyphenyl)porphine	0.612(0.056)	0.21	0.17	0.04
19	5-( <i>p</i> -chlorophenyl)-10,15,20-tris( <i>p</i> -carboxyphenyl)porphine	0.758(0.188)	0.12	0.19	-0.07
20	5-( <i>p</i> -carboxyphenyl)-10,15,20-tritolylporphine	14.659(2.585)	-1.17	-1.20	0.03
21	<i>meso</i> -tetrakis(4-carboxamidophenyl)porphine	1.075(0.369)	-0.03	-0.08	0.05
22 <sup>b,d</sup>	aurintricarboxylic acid (ATA)	28.4			
23 <sup>b,d</sup>	hemin	35.3			

<sup>a</sup> Calculated anti-HIV-1 activities were based on the "fitted model". <sup>b</sup> These data points were not used to derive the model. <sup>c</sup> Concentration (μM) at which the production of the HIV-1 core protein P24 was reduced to 50% of that detected in HIV-1 infected cultures in the absence of porphyrins. <sup>d</sup> Data from ref 22.

**Figure 3.** Stereoview of 21 superimposed porphyrin analogs.**Figure 4.** Plot of observed vs calculated anti-HIV-1 activity.

was also investigated and yielded poorer correlations ( $r^2_{cv} = 0.539$  and  $S_{cv} = 0.516$ ;  $r^2_{cv} = 0.457$  and  $S_{cv} = 0.560$ ;  $r^2_{cv} = 0.469$  and  $S_{cv} = 0.554$ , respectively).

This CoMFA study identified several favorable electrostatic interaction sites, three of which are located almost across the three meso-carbon atoms of tetraphenyl porphyrins. There is no region across the fourth meso carbon

atoms for favorable or unfavorable electrostatic interactions (Figure 5). This brings about one important question, i.e., how many carboxylic acid groups on the phenyl rings of *meso*-tetraphenylporphine type compounds are required for optimal anti-HIV-1 activity? According to the electrostatic contour, three carboxylic acid groups are sufficient to produce good activity. In fact, 5-phenyl-10,15,20-tris(*p*-carboxyphenyl)porphine (18) has the highest activity among all the compounds tested. Another tricarboxylic acid containing compound, 5-(*p*-chlorophenyl)-10,15,20-tris(*p*-carboxyphenyl)porphine (19), is also one of the most active compounds. However, one tetracarboxylic acid containing compound, *meso*-tetrakis(4-carboxyphenyl)porphine (16) has activity similar to the tricarboxy compounds. All of the carboxylic acid groups are symmetrical in this compound, and probably only three carboxyls are taking part in receptor binding.

*meso*-Tetraphenylporphine (15) has no carboxylic acid groups and is one of the weakly active compounds in that series. There are several polycarboxylic acids containing

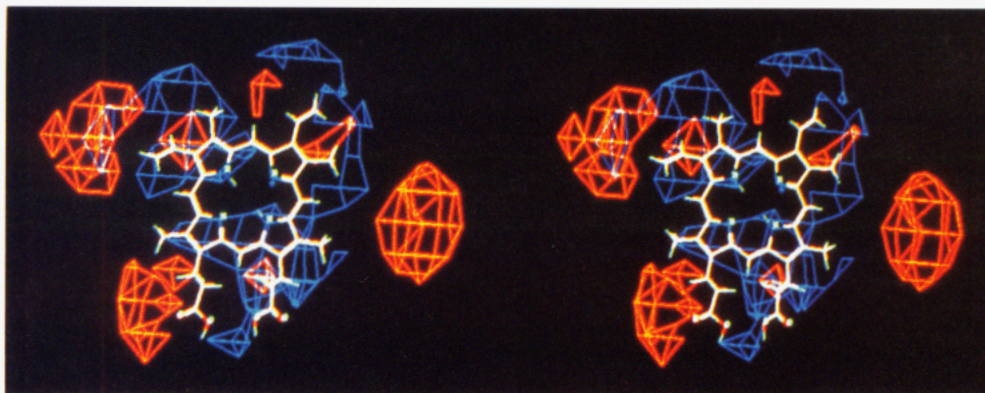


**Figure 5.** Stereoview of the contour plot of electrostatic fields. The contours were drawn at the 0.005 level. Protoporphyrin IX is shown as the reference molecule.

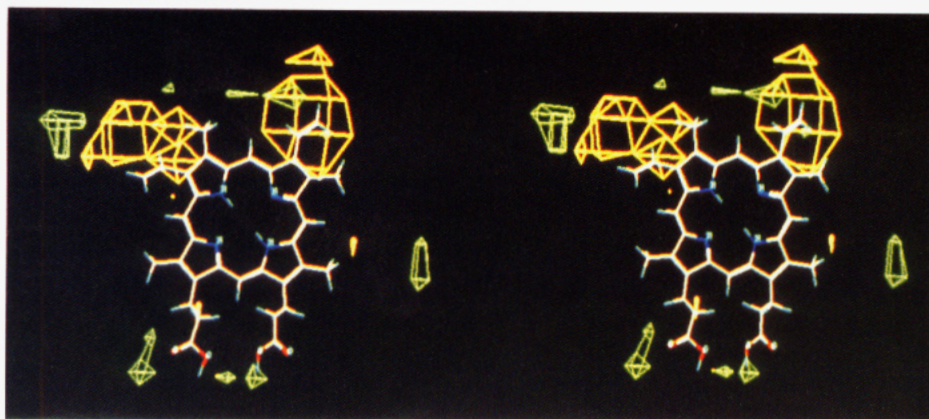


**Figure 6.** Stereoview of the contour plot of steric fields. The contours were drawn at the 0.007 level. Protoporphyrin IX is shown as the reference molecule.

**Table 5.** Frequency of Occurrences of Positively Charged and Hydrophobic Amino Acid (AA) Residues in 217 V3 Loop Sequences

	1										2										3																			
	1	2	3	4	5	6	7	8	9	0	1	2	3	4	5	6	7	8	9	0	1	2	3	4	5	6	7	8	9	0										
	C	T	R	P	.	N	N	N	T	R	K	S	.	.	I	H	I	G	P	G	R	A	F	Y	T	T	G	E	I	I	G	D	I	R	Q	A	H	C <sup>a</sup>		
% Occurrence of Positively Charged AA (R,K)	100										93 75										55										95									
% Occurrence of Hydrophobic AA (I, F, Y, V, M, W)											90 98										99 94										94 91 99									

<sup>a</sup> Dots indicate deletions in the consensus sequence as compared with other sequences. Amino acid sequence of the consensus V3 loop corresponding to North American/European HIV-1 isolates (= subgroup B).<sup>49</sup>

compounds, e.g., 8–12, which do not quite satisfy the requirement for favorable electrostatic interaction, and all of them have low antiviral activity. Protoporphyrin IX (1) and its *N*-methyl derivative (2) interact principally through their propionic acid groups, providing favorable electrostatic interactions and their two vinyl groups providing favorable positive steric interactions as evident from Figure 6, and represent two of the most active compounds in that series.

The contour plots (Figure 5 and 6) also indicate that one of the favorable electrostatic interaction sites and two of the favorable steric interaction sites are located near one of the carboxylic acid groups and the vinyl groups of

protoporphyrin IX, respectively. This is consistent with our starting pharmacophore hypothesis used for systematic conformational searches.

## Discussion

Comparative molecular field analysis (CoMFA) methodology has shown its potential in a number of studies on structure–activity analysis.<sup>42–48</sup> We have applied CoMFA successfully to a set of 21 porphyrin derivatives with anti-HIV-1 activity targeted to the V3 loop of the HIV-1 gp120 envelope glycoprotein. A high cross-validated  $r^2_{cv}$  with a significantly high correlation coefficient of the “fitted model” and a low standard error of estimate suggest that

this model could be used as a predictive tool for further anti-HIV-1 drug development of porphyrin type compounds. The CoMFA analysis clearly revealed key structural aspects of the porphyrin derivatives required for anti-HIV-1 activity. The electrostatic contour plot indicates that *meso*-tetraphenylporphine type compounds require at least three carboxylic acid groups on the phenyl ring for appreciable anti-HIV-1 activity. We have included one monocarboxylic acid derivative, 5-(*p*-carboxyphenyl)-10,15,20-tritolyldiporphine (**20**), which has much poorer activity than any of the tri- or tetracarboxy compounds of this class (approximately 30 times less active). These results suggest that there could be at least three major positively charged interaction sites present on the "receptor", i.e., on the V3 loop, for favorable interaction with the negatively charged carboxylic acid groups. Steric contour plots also indicate both favorable and unfavorable steric effects.

We analyzed the occurrence of positively charged (e.g., arginine and/or lysine) and hydrophobic (e.g., isoleucine, valine, phenylalanine, tyrosine, methionine, tryptophan, etc.) amino acid residues in 217 V3 loop sequences reflecting a global variation of this region of the HIV-1 gp120 envelope glycoprotein.<sup>49</sup> The result of the analysis is shown in Table 5 and indicates that the positions within the V3 loop sequence of positively charged and hydrophobic amino acid residues, respectively, are highly conserved notwithstanding the recognized hypervariability of this segment of gp120. This might justify our CoMFA-derived model and our hypothesis that some of these positively charged and hydrophobic amino acid residues in the V3 loop contribute to the binding of structurally varied porphyrin derivatives having anionic and hydrophobic binding sites. This binding may lead to distortion of the conformation of the V3 loop and consequently also of sterically adjacent regions in the gp120 envelope glycoprotein. This could lead to interference with viral entry and syncytium formation and thus to inhibition of virus replication. Porphyrins did not bind to a deletion mutant of gp120 lacking the V3 loop sequence<sup>50</sup> (own data to be published).

We expect that the model presented here will be a useful guiding tool for further design of porphyrin type compounds in anti-HIV-1 drug development.

**Acknowledgment.** This work was supported by a Grant CA43315 from the National Institutes of Health. We thank Dr. J. F. Marecek of the Chemical Synthesis Center, State University of New York, Stony Brook, NY, for synthesizing compound **20**, Dr. A. K. Ghose of Sterling-Winthrop for his helpful suggestions on conformational searches, and R. Ratner for help in preparing the manuscript and some of the figures.

**Supplementary Material Available:** Coordinates and connection table for all 21 porphyrin derivatives in Sybyl MOL2 file format (75 pages). Ordering information is given on any current masthead page.

## References

- (1) Larder, B. A.; Darby, G.; Richman, D. D. HIV with reduced sensitivity to zidovudine (AZT) isolated during prolonged therapy. *Science* **1989**, *243*, 1731-1734.
- (2) St. Clair, M. H.; Martin, J. L.; Tudor-Williams, G.; Bach, M. C.; Vavro, C. L.; King, D. M.; Kellam, P.; Kemp, S. D.; Larder, B. A. Resistance to ddI and sensitivity to AZT induced by a mutation in HIV-1 reverse transcriptase. *Science* **1991**, *253*, 1557-1559.
- (3) Montaner, J. S. G.; Singer, J.; Schechter, M. T.; Raboud, J. M.; Tsoukas, C.; O'Shaughnessy, M.; Ruedy, J.; Nagai, K.; Salomon, H.; Spira, B.; Wainberg, M. A. Clinical correlates of *in vitro* HIV-1 resistance to zidovudine. Results of the multicentre Canadian AZT trial. *AIDS* **1993**, *7*, 189-196.
- (4) Richman, D. D.; Fischl, M. A.; Grieco, M. H.; Gottlieb, M. S.; Volberding, P. A.; Laskin, O. L.; Leedom, J. M.; Groopman, J. E.; Mildvan, D.; Hirsch, M. S.; Jackson, G. G.; Durack, D. T.; Nusinoff-Lehrman, S. AZT Collaborative Working Group. The toxicity of azidothymidine (AZT) in the treatment of patients with AIDS and AIDS-related complex. *N. Engl. J. Med.* **1987**, *317*, 192-197.
- (5) Dainiak, N.; Worthington, M.; Riordan, M. A.; Kreczko, S.; Goldman, L. 3'-azido-3'-deoxythymidine (AZT) inhibits proliferation *in vitro* of human haematopoietic progenitor cells. *Br. J. Haematol.* **1988**, *69*, 299-304.
- (6) Gallicchio, V. S.; Hughes, N. K.; Hulet, B. C. In vitro modulation of the toxicity associated with the use of zidovudine on normal murine, human, and murine retrovirus-infected hematopoietic progenitor stem cells with basic fibroblast growth and synergistic activity with interleukin-1. *J. Leukoc. Biol.* **1992**, *51*, 336-342.
- (7) Aboulker, J.-P.; Swart, A. M. Preliminary analysis of the Concorde trial. *Lancet* **1993**, *341*, 889-890.
- (8) Neurath, A. R.; Strick, N.; Haberfield, P.; Jiang, S. Rapid prescreening for antiviral agents against HIV-1 based on their inhibitory activity in site-directed immunoassays. II. Porphyrins reacting with the V3 loop of gp120. *Antiviral Chem. Chemother.* **1992**, *3*, 55-63.
- (9) Mahmood, N.; Moore, P. S.; De Tommasi, N.; De Simone, F.; Colman, S.; Hay, A. J.; Pizarro, C. Inhibition of HIV infection by caffeoylquinic acid derivatives. *Antiviral Chem. Chemother.* **1993**, *4*, 235-240.
- (10) Smallheer, J. M.; Otto, M. J.; Amaral-Ly, C. A.; Earl, R. A.; Myers, M. J.; Pennev, P.; Montefiori, D. C.; Wuonola, M. A. Synthesis and anti-HIV activity of a series of 2-indolinones and related analogues. *Antiviral Chem. Chemother.* **1993**, *4*, 27-39.
- (11) Moriya, T.; Saito, K.; Kurita, H.; Matsumoto, K.; Otake, T.; Mori, H.; Morimoto, M.; Ueba, N.; Kunita, N. A new candidate for an anti-HIV-1 agent: Modified cyclodextrin sulfate (mCDS71). *J. Med. Chem.* **1993**, *36*, 1674-1677.
- (12) Mohan, P.; Wong, M. F.; Verma, S.; Huang, P. P.; Wickramasinghe, A.; Baba, M. Structure-activity relationship studies with symmetric naphthalenesulfonic acid derivatives. Synthesis and influence of spacer and naphthalenesulfonic acid moiety on anti-HIV-1 activity. *J. Med. Chem.* **1993**, *36*, 1996-2003.
- (13) De Clercq, E. Basic Approaches to Anti-retroviral treatment. *J. Acquired Immune Defic. Syndr.* **1991**, *4*, 207-218.
- (14) Mitsuya, H.; Yarchoan, R.; Broder, S. Molecular targets for AIDS therapy. *Science* **1990**, *249*, 1533-1544.
- (15) Maddon, P. J.; Dagleish, A. G.; McDougal, J. S.; Clapham, P. R.; Weiss, R. A.; Axel, R. The T4 gene encodes the AIDS virus receptor and is expressed in the immune system and the brain. *Cell* **1986**, *47*, 333-348.
- (16) Tersmette, M.; Van Dongen, J. J. M.; Clapham, P. R.; De Goede, R. E. Y.; Wolvers-Tettero, I. L. M.; Geurts Van Kessel, A.; Huisman, J. G.; Weiss, R. A.; Miedema, F. Human immunodeficiency virus infection studied in CD4-expressing human-murine T-cell hybrids. *Virology* **1989**, *168*, 267-273.
- (17) Ivanoff, L. A.; Looney, D. J.; McDanal, C.; Morris, J. F.; Wong-Staal, F.; Langlois, A. J.; Petteway, S. R., Jr.; Matthews, T. J. Alteration of HIV-1 infectivity and neutralization by a single amino acid replacement in the V3 loop domain. *AIDS Res. Hum. Retroviruses* **1991**, *7*, 595-603.
- (18) Page, K. A.; Stearns, S. M.; Littman, D. R. Analysis of mutations in the V3 domain of gp160 that affect fusion and infectivity. *J. Virol.* **1992**, *66*, 524-533.
- (19) Javaherian, K.; Langlois, A. J.; McDanal, C.; Ross, K. L.; Eckler, L. I.; Jellis, C. L.; Profy, A. T.; Rusche, J. R.; Bolognesi, D. P.; Putney, S. D.; Matthews, T. J. Principal neutralizing domain of the human immunodeficiency virus type 1 envelope protein. *Proc. Natl. Acad. Sci. U.S.A.* **1989**, *86*, 6768-6772.
- (20) Palker, T. J.; Clark, M. E.; Langlois, A. J.; Matthews, T. J.; Weinhold, K. J.; Randall, R. R.; Bolognesi, D. P.; Haynes, B. F. Type-specific neutralization of the human immunodeficiency virus with antibodies to *env*-encoded synthetic peptides. *Proc. Natl. Acad. Sci. U.S.A.* **1988**, *85*, 1932-1936.
- (21) Kenealy, W. R.; Matthews, T. J.; Ganfield, M.-C.; Langlois, A. J.; Waselefsky, D. M.; Petteway, S. R., Jr. Antibodies from human immunodeficiency virus-infected individuals bind to a short amino acid sequence that elicits neutralizing antibodies in animals. *AIDS Res. Hum. Retroviruses* **1989**, *5*, 173-182.
- (22) Neurath, A. R.; Haberfield, P.; Joshi, B.; Hewlett, I. K.; Strick, N.; Jiang, S. Rapid prescreening for antiviral agents against HIV-1 based on their inhibitory activity in site-directed immunoassays. I. The V3 loop of gp120 as target. *Antiviral Chem. Chemother.* **1991**, *2*, 303-312.
- (23) Levere, R. D.; Gong, Y.-F.; Kappas, A.; Bucher, D. J.; Wormser, G. P.; Abraham, N. G. Heme inhibits human immunodeficiency virus 1 replication in cell cultures and enhances the antiviral effect of zidovudine. *Proc. Natl. Acad. Sci. U.S.A.* **1991**, *88*, 1756-1759.

- (24) Jackson, A. H. N-substituted porphyrins and corroles. In *The Porphyrins, Volume 1, Structure and Synthesis, Part A*; Dolphin, D., Ed.; Academic Press: New York, 1978; pp 340-364.
- (25) Milgrom, L. R. Synthesis of some new tetra-aryl porphyrins for studies in solar energy conversion. Part 2. Asymmetric porphyrins. *J. Chem. Soc., Perkin Trans. 1* 1984, 1483-1487.
- (26) Morrison, R. T. and Boyd, R. N., *Organic Chemistry*, 3rd ed.; Allyn and Bacon, Inc.: Boston, 1976; p 591.
- (27) Achar, B. N.; Fohlen, G. M.; Parker, J. A.; Keshavayya, J. Synthesis and structural studies of metal (II) 4,9,16,23-phthalocyanine tetraamines. *Polyhedron* 1987, 6, 1463-1467.
- (28) Anton, J. A.; Kwong, J.; Loach, P. A. Synthesis of covalently linked porphyrin dimers and trimers (1). *J. Heterocycl. Chem.* 1976, 13, 717-725.
- (29) Jiang, S.; Lin, K.; Neurath, A. R. Enhancement of human immunodeficiency virus type 1 infection by antisera to peptides from the envelope glycoproteins gp120/gp41. *J. Exp. Med.* 1991, 174, 1557-1563.
- (30) SYBYL Molecular Modeling System (Version 6.01); Tripos Associates, Inc.: St. Louis, MO.
- (31) Caughey, W. S.; Ibers, J. A. Crystal and molecular structure of the free base porphyrin, protoporphyrin IX dimethyl ester. *J. Am. Chem. Soc.* 1977, 99, 6639-6645.
- (32) Fischer, M. S.; Templeton, D. H.; Zalkin, A.; Calvin, M. Crystal and molecular structure of methyl pheophorbide with applications to the chlorophyll arrangement in photosynthetic lamellae. *J. Am. Chem. Soc.* 1972, 94, 3613-3619.
- (33) Robertson, J. M. An X-ray study of the phthalocyanines. Part II. Quantitative structure determination of the metal-free compound. *J. Chem. Soc.* 1936, 1195-1209.
- (34) Silvers, S. J.; Tulinsky, A. Triclinic tetraphenylporphyrin. *J. Am. Chem. Soc.* 1967, 89, 3331-3337.
- (35) Clark, M.; Cramer, R. D., III; Van Opdenbosch, N. Validation of the general purpose Tripos 5.2 force field. *J. Comput. Chem.* 1989, 10, 982-1012.
- (36) Marshall, G. R.; Barry, C. D.; Bosshard, H. E.; Dammkoehler, R. A.; Dunn, D. A. The conformational parameter in drug design: The active analog approach. In *Computer-Assisted Drug Design*; Olson, E. C., Christoffersen, R. E., Eds.; American Chemical Society: Washington, DC, 1979; pp 205-226.
- (37) Mayer, D.; Naylor, C. B.; Motoc, I.; Marshall, G. R. A unique geometry of the active site of angiotensin-converting enzyme consistent with structure-activity studies. *J. Comput.-Aided Mol. Des.* 1987, 1, 3-16.
- (38) Dewar, M. J. S.; Zoebisch, E. G.; Healy, E. F.; Stewart, J. J. P. AM1: A new general purpose quantum mechanical molecular model. *J. Am. Chem. Soc.* 1985, 107, 3902-3909.
- (39) Lindberg, W.; Persson, J.-A. Partial least-squares method for spectrofluorimetric analysis of mixtures of humic acid and ligninsulfonate. *Anal. Chem.* 1983, 55, 643-648.
- (40) Cramer, R. D., III; Bunce, J. D.; Patterson, D. E.; Frank, I. E. Crossvalidation, bootstrapping, and partial least squares compared with multiple regression in conventional QSAR studies. *Quant. Struct.-Act. Relat.* 1988, 7, 18-25.
- (41) SYBYL 6.0 Theory Manual, 1992; Tripos Associates: St. Louis, MO, 1992; p 2253.
- (42) Cramer, R. D., III; Patterson, D. E.; Bunce, J. D. Comparative molecular field analysis (CoMFA). 1. Effect of shape of binding of steroids to carrier proteins. *J. Am. Chem. Soc.* 1988, 110, 5959-5967.
- (43) Kim, K. H. Nonlinear dependence in comparative molecular field analysis. *J. Comput.-Aided Mol. Des.* 1993, 7, 71-82.
- (44) Wong, G.; Koehler, K. F.; Skolnick, P.; Gu, Z.-Q.; Ananthan, S.; Schönholzer, P.; Hunkeler, W.; Zhang, W.; Cook, J. M. Synthetic and computer-assisted analysis of the structural requirements for selective, high-affinity ligand binding to diazepam-insensitive benzodiazepine receptors. *J. Med. Chem.* 1993, 36, 1820-1830.
- (45) Klebe, G.; Abraham, U. On the prediction of binding properties of drug molecules by comparative molecular field analysis. *J. Med. Chem.* 1993, 36, 70-80.
- (46) Calder, J. A.; Wyatt, J. A.; Frenkel, D. A.; Casida, J. E. CoMFA validation of the superposition of six classes of compounds which block GABA receptors non-competitively. *J. Comput.-Aided Mol. Des.* 1993, 7, 45-60.
- (47) Debnath, A. K.; Hansch, C.; Kim, K. H.; Martin, Y. C. Mechanistic interpretation of the genotoxicity of nitrofurans (antibacterial agents) using quantitative structure-activity relationships and comparative molecular field analysis. *J. Med. Chem.* 1993, 36, 1007-1016.
- (48) Langer, T.; Wermuth, C. G. Inhibitors of prolyl endopeptidase: Characterization of pharmacophoric pattern using conformational analysis and 3D-QSAR. *J. Comput.-Aided Mol. Des.* 1993, 7, 253-262.
- (49) Myers, G.; Korber, B.; Berzofsky, J. A.; Smith, R. F. *Human retroviruses and AIDS 1992*; Los Alamos National Laboratory: Los Alamos, NM, 1992.
- (50) Wyatt, R.; Thali, M.; Tilley, S.; Pinter, A.; Posner, M.; Ho, D.; Robinson, J.; Sodroski, J. Relationship of the human immunodeficiency virus type 1 gp120 third variable loop to a component of the CD4 binding site in the fourth conserved region. *J. Virol.* 1992, 66, 6997-7004.